



# HHS Public Access

Author manuscript

*Biochemistry*. Author manuscript; available in PMC 2017 July 16.

Published in final edited form as:

*Biochemistry*. 2003 November 11; 42(44): 12805–12812. doi:10.1021/bi035370p.

## Lecithin Retinol Acyltransferase Is a Founder Member of a Novel Family of Enzymes†

Wan Jin Jahng<sup>‡</sup>, Linlong Xue<sup>‡</sup>, and Robert R. Rando<sup>\*</sup>

Department of Biological Chemistry and Molecular Pharmacology, Harvard Medical School, 45 Shattuck Street, Boston, Massachusetts 02115

### Abstract

Lecithin retinol acyltransferase (LRAT) catalyzes the reversible esterification of vitamin A using lecithin as the acyl donor. LRAT is the founder member of a new class of enzymes, which include class II tumor suppressors, proteins essential for development, and putative proteases. All of these proteins possess Cys and His residues homologous to C161 and H60 of LRAT. These two residues are shown here to be essential for LRAT activity and are part of a catalytic dyad reminiscent of that found in thiol proteases. However, the local primary sequence contexts of C161 and H60 of LRAT and family are not at all homologous to those found in the approximately 20 thiol protease families. Moreover, LRAT shows p*K*s of 8.3 and 10.8, compared to approximately 4.0 and 8.5 observed in the thiol proteases. LRAT also contains Gln177 and Asp67 residues, which are largely conserved in the homologues. However, neither of these residues is essential for catalysis. Thiol proteases often contain catalytically essential Asp or Gln residues. It is concluded that LRAT is the founder member of a new class of Cys-His enzymes with diverse functions.

Lecithin retinol acyltransferase (LRAT)<sup>1</sup> catalyzes the reversible acylation of vitamin A (all-*trans*-retinol) using lecithin as the acyl donor to generate all-*trans*-retinyl esters (Scheme 1) (1–4). LRAT is essential for human vision because it catalyzes the formation of the substrate for isomerohydrolase, which produces 11-*cis*-retinol, the direct precursor of 11-*cis*-retinal, the visual chromophore (4). The enzyme is found in tissues other than the eye and is likely to be generally involved in vitamin A storage and mobilization (5). LRAT is an integral membrane protein which associates with retinal pigment epithelial (RPE) membranes in the vertebrate visual system (1–4). Although the enzyme has been solubilized and partially purified, it has never been purified to homogeneity from RPE membranes, as it becomes exceedingly labile as a consequence of extensive purification (6). Nonetheless, LRAT has been identified and characterized through use of specific affinity labeling agents, such as all-*trans*-retinyl bromoacetate (RBA) and *N*-Boc-L-biotinyl-11-aminoundecane chloromethyl ketone (BACMK), which yielded partial sequence information (Scheme 2) (7, 8). The

<sup>†</sup>The work described herein was supported by the U.S. Public Health Service, NIH Grant EY-04096.

<sup>\*</sup>To whom correspondence should be addressed: 617-432-1794 (tel); 617-432-0471 (fax); robert\_rando@hms.harvard.edu.

<sup>‡</sup>These authors contributed equally to this work.

<sup>1</sup>Abbreviations: BACMK, *N*-Boc-L-biotinyl-11-aminoundecane chloromethyl ketone; BRCA, 3-[*N*-Boc-Lys(biotinyl)-*O*]-all-*trans*-retinyl chloroacetate; ECL, enhanced chemiluminescence; HRP, horseradish peroxidase; LRAT, lecithin retinol acyltransferase; RBA, all-*trans*-retinyl bromoacetate; RCA, all-*trans*-retinyl chloroacetate; RPE, retinal pigment epithelium; RP-HPLC, reversed-phase high-performance liquid chromatography; SDS-PAGE, sodium dodecyl sulfate-polyacrylamide gel electrophoresis; TFA, trifluoroacetic acid; tLRAT, truncated lecithin retinol acyltransferase.

cloning and sequencing of LRAT showed it to be the founder member (4, 7) of an expanding family of homologous proteins which include class II tumor suppressors (9, 10), putative viral proteases (11), and EGL-26, an enzyme that mediates morphogenesis in *Caenorhabditis elegans* (12) (Scheme 3). All of these proteins contain conserved residues corresponding to C161 and H60 of LRAT, and most of them contain conserved residues corresponding to Q177 and D67 of LRAT (Scheme 3). Importantly, LRAT is the only member of this family whose biochemical function is known.

Since the function of LRAT is known, it is of substantial interest to uncover the mechanistic class to which it belongs, as this will also inform biochemical investigations on its homologues. Both full-length human LRAT and a truncated version, tLRAT, have been prepared and expressed (7, 13). The N- and C-terminal transmembrane segments (1–30, 197–230) are truncated in tLRAT, and a His tag is added, making possible the overexpression and purification of the enzyme from bacteria (13). The ready availability of tLRAT makes site-specific mutagenic and further biochemical studies on the protein possible.

To help to define the mechanistic class of enzymes to which LRAT belongs, it is important to determine which amino acid residues, among the conserved group, are essential for catalysis. In the family of homologues shown in Scheme 3, both C161 and H60 are completely conserved, and Q177 and D67 are largely conserved (Scheme 3). Previous studies have shown that, in full-length expressed human LRAT, both C161A and C168A are enzymatically inactive, while C161S is essentially inert and C168S is substantially active (14). The remaining two Cys residues are mutated with little consequence on catalysis (14). Of the six His residues of LRAT, only H60 is uniquely conserved. Previous studies had shown that H46Q, H72Q, and H126Q are all active in full-length human LRAT (15). H163Q proved to be inert in this series, probably because this mutation perturbs the C161, a Cys residue important for LRAT catalysis.

In the current studies a combination of affinity-labeling experiments and site-specific mutagenic experiments is used to demonstrate that C161 is the essential catalytic thiol residue of LRAT and that H60 is also essential for catalysis. These two residues form the essential catalytic dyad of LRAT. This catalytic dyad could possibly represent a novel thiol protease motif, which functions in the case of LRAT in an acyltransferase reaction. In addition, conserved residues Q177 and D67 may have a role to play in catalysis, but site-specific mutagenesis shows them not to be essential.

## EXPERIMENTAL PROCEDURES

### Materials

The syntheses of RBA, BRCA, and BACMK are described elsewhere (7, 12, 16). Frozen bovine eye cups were obtained from W. L. Lawson Co. (Lincoln, NE). Western blot blocking buffer, Gel-code blue, neutravidin, and Tris-buffered saline pack (25 mM Tris, 150 mM NaCl, pH 7.2) were from Pierce. HPLC grade solvents were from J. T. Baker. Coomassie brilliant blue R-250 was from Bio-Rad. The silver staining kit, poly(vinylidene fluoride) membrane, anti-rabbit Ig-conjugated horseradish peroxidase, and ECL-Western blotting kit

were from Amersham Pharmacia Biotech. Precast gels (4–20%, 8 cm × 8 cm) for SDS-PAGE were from Invitrogen Life Technologies. Benchmark prestained markers were from Gibco BRL Life Technologies. Biotinylated molecular weight markers, two-color prestained markers, avidin-conjugated horseradish peroxidase, and 10× Tris-buffered saline solution (20 mM Tris, 500 mM NaCl, pH 7.5) were from Bio-Rad. [11,12-<sup>3</sup>H<sub>2</sub>]-all-*trans*-retinol was obtained from NEN Life Sciences. L- $\alpha$ -Dipalmitoylphosphatidylcholine (DPPC), bovine serum albumin (BSA), and dithiothreitol (DTT) were from Sigma. The QuikChange site-directed mutagenesis kit was purchased from Stratagene. The GeneAmp XL PCR kit was from Applied Biosystem Inc. *Eco*RI and T4 DNA ligase were from New England Biolabs. Anti-LRAT antibody was a generous gift provided by Prof. Dean Bok (UCLA). All other reagents were of analytical grade.

## Methods

**Specific Labeling of tLRAT by RCA, BRCA, and BACMK**—Affinity labeling protocols were described elsewhere (7, 12, 17). Briefly, all labeling experiments using retinoids were performed in a dark room under dim red light. Generally, 100  $\mu$ g of purified tLRAT (1 mg/mL) was incubated with the reagent (10  $\mu$ M) for 1 h at 4 °C. At the end of the incubation period, excess reagent was removed by dialysis (MW cutoff 5 kDa) or acetone precipitation (1 mL, -20 °C). The labeled sample was applied to a SDS-PAGE. Tris-glycine-polyacrylamide gel (4–20%, 8 cm × 8 cm) electrophoresis was carried out using Tris (25 mM), glycine (192 mM), and SDS (0.1%) running buffer. Protein denaturation was performed by heating samples (100 °C, 2 min) in sample buffer (2×) containing SDS (4%), 2-mercaptoethanol (10%), glycerol (20%), bromophenol blue (0.004%) and Tris (125 mM, pH 6.8). Proteins were visualized by Coomassie blue staining (0.1%) or silver staining. Proteins were digested by trypsin and/or chymotrypsin (1  $\mu$ g for in-gel digestion; 1/20th of the sample for in-solution digestion) in 50 mM ammonium bicarbonate buffer overnight at 37 °C. For purification of [11,12-<sup>3</sup>H<sub>2</sub>]RCA (2) labeled tLRAT peptide, reversed-phase high-performance liquid chromatography (RP-HPLC) was performed on a C18 column (Vydac 218TP52) at the Core facility at Dana-Farber Cancer Institute (Boston, MA). The peptides were eluted with a linear gradient from 0 to 70% acetonitrile with 0.1% TFA. Fractions were collected every minute (50  $\mu$ L), and radioactivity was monitored by scintillation counting (Beckman LS6500) using Ultima Gold (Packard Bioscience) scintillation cocktail. Digested peptides labeled by BRCA (3) and BACMK (4) were incubated with neutravidin-agarose beads overnight at room temperature, followed by washing five times with sodium phosphate buffer (20 mM, 150 mM NaCl, pH 7.5) before elution. Biotinylated peptide by BRCA (3) was eluted from the beads by incubation of sodium carbonate/bicarbonate buffer (200 mM, pH 11) overnight whereas biotinylated peptide by BACMK (4) was eluted by 8 M guanidine hydrochloride. Eluted peptide was purified by a C18 column (Waters) twice using an acetonitrile gradient elution buffer (0–90% MeCN, 0.1% TFA) prior to mass spectrometric analysis.

**Western Blot Analysis**—The preparation of polyclonal anti-LRAT peptide/protein antibodies was reported previously (7, 13). After protein separation by SDS-PAGE, proteins were transferred to a poly(vinylidene fluoride) (PVDF) membrane for 30 min at 15 V using Tris-glycine buffer (25 mM Tris, 192 mM glycine) and ethanol (20%) by semidry transfer

apparatus (Bio-Rad). The membrane was blocked with 5% nonfat dried milk or super block blocking buffer (Pierce, 3% BSA) for 2 h at room temperature. Anti-LRAT antibody (1:4000 dilution, 2 h), anti-rabbit Ig-linked horseradish peroxidase (1:8000 dilution, 1 h) from donkey, and the enhanced chemiluminescence (ECL) system were used to detect the tLRAT band.

**Biotin Detection Blot Analysis**—After protein separation by SDS-PAGE, proteins were transferred to poly(vinylidene fluoride) (PVDF) membranes. Membranes were blocked in the blocking solution (100 mL, 3% gelatin, 25 mM Tris, 150 mM NaCl, pH 7.2) using a shaker platform for 1 h. The blocking solution was removed, and the membrane was washed twice with TTBS solution (0.05% Tween 20, 25 mM Tris, 150 mM NaCl, pH 7.2) for 5 min. After removal of the TTBS buffer, avidin-conjugated horseradish peroxidase (33  $\mu$ L) in antibody buffer (100 mL, 1% gelatin, 0.05% Tween 20, 25 mM Tris, 150 mM NaCl, pH 7.2) was applied for 1 h. The membrane was washed twice with TTBS (100 mL, 0.05% Tween 20, 25 mM Tris, 150 mM NaCl, pH 7.2) for 5 min and twice by TBS (100 mL, 25 mM Tris, 150 mM NaCl, pH 7.2) for 5 min. ECL solution (6 mL) was added into the membrane for 1 min before X-ray film exposure. Using a higher concentration of saline TTBS buffer (20 mM Tris, 0.05% Tween 20, 500 mM NaCl, pH 7.5) reduced the background signal and endogenously biotinylated protein bands.

**Mass Spectrometry Analysis**—The method used for trypsin digestion followed by mass spectrometric analysis of labeled proteins was described in detail elsewhere (17). Briefly, the gel containing the labeled protein was dehydrated in MeCN for 10 min. Gel pieces were covered with DTT (10 mM) in  $\text{NH}_4\text{HCO}_3$  (100 mM) to reduce proteins for 1 h at 56 °C. After being cooled to room temperature, the reducing buffer was removed. The gel washing/dehydration cycle was repeated three times with  $\text{NH}_4\text{HCO}_3$ /MeCN before trypsin (12.5 ng/ $\mu$ L, 5  $\mu$ L/ $\text{mm}^2$  gel, overnight) and/or chymotrypsin digestion at 37 °C. Gel slices were centrifuged, and the supernatant was collected. Peptides were further extracted by one change of 20 mM  $\text{NH}_4\text{HCO}_3$  and three changes of 5% formic acid in 50%  $\text{CH}_3\text{CN}$  (20 min between changes) at 25 °C. Trypsin digestion of the gel band and the mass spectrometric analysis were performed at the Taplin Biological Mass Spectrometry Facility at Harvard Medical School (Boston, MA) and the Harvard Microchemistry Facility (Cambridge, MA). When peptides were analyzed by iontrap mass spectrometry (LCQ DECA, ThermoFinnigan), the amino acid sequence was determined by tandem mass spectrometry (MS/MS) and database search. For microcapillary LC elution, a linear gradient of 100% of buffer A [MeCN (5%),  $\text{H}_2\text{O}$  (95%), formic acid (0.1%), heptafluorobutyric acid (0.005%)] through 100% of buffer B [MeCN (95%),  $\text{H}_2\text{O}$  (5%), formic acid (0.1%), heptafluorobutyric acid (0.005%)] was used. The capillary column was 75  $\mu$ m i.d.  $\times$  12 cm bed length. The flow rate was split down from the pumps to 200 nL/min for the separation. The bovine database was extracted and downloaded by FTP from the NCBI web site (<http://www.ncbi.nlm.nih.gov/>). MALDI-TOF mass analysis was performed using Voyager-DE STR from Applied Biosystems at the Dana-Farber Cancer Institute Core Facility (Boston, MA).  $\alpha$ -Cyano-4-hydroxycinnamic acid (0.5  $\mu$ L, 10 mg/mL) was used as the matrix for each sample (0.5  $\mu$ L). In the reflector mode, 20000 V of accelerating voltage and 200 ns of extraction delay time were applied. The laser intensity was 1900–2300, and 100–200 laser

shots were collected for each spectrum. The acquisition mass range was 750–4500 Da with a 600 Da low mass gate.

**Kinetic Analysis of Retinyl Ester Formation**—For LRAT and mutants, steady-state kinetic measurements were performed to obtain the  $K_M$  and  $V_{max}$  (13). For tLRAT and mutants, all-*trans*-retinyl ester formation was measured using 0.2  $\mu$ M [11,12- $^3$ H $_2$ ]-all-*trans*-retinol as substrate. All activity assays were performed as previously described (13).

**Site-Directed Mutagenesis**—tLRAT mutants were prepared using a QuikChange site-directed mutagenesis kit (Stratagene Inc.) according to the vendor's instruction with minor modification. For full-length LRAT, H57Q and H60Q were generated by the overlapping extension (7).

**Protein Expression and Purification**—LRAT and the mutants were expressed in human kidney cells HEK 293 as described elsewhere (7). For tLRAT and the mutants, the plasmids were transformed into *Escherichia coli* BL21STAR-(DE3) for expression. Briefly, the cells were incubated in LB media containing 1 mg/L ampicillin at 37 °C with shaking at 275 rpm. When the OD reached 0.8, IPTG (final concentration 1 mM) was added to induce expression. Cells were harvested 4–6 h after induced expression and stored at –80 °C. The expressed protein was extracted with 1% SDS at room temperature after the cells were lysed either with lysozyme or by sonication. Protein purification was accomplished by applying the SDS extract directly onto a Ni column as described (13).

## RESULTS

### C161 Is the Active Site Nucleophile of LRAT

Previous site-specific mutagenic experiments identified the importance of C161 and C168 for catalysis in LRAT (14). To unambiguously identify which Cys residue is the active site, nucleophile active site mapping on affinity-labeled tLRAT was performed. To verify that labeling is irreversible and specific, purified tLRAT was inactivated with  $^3$ H-labeled RCA (specific activity 50  $\mu$ Ci/mmol). Labeling of tLRAT with [11,12- $^3$ H $_2$ ]RCA (**2**) clearly shows covalent modification of the protein. [11,12- $^3$ H $_2$ ]RCA labeling of tLRAT, SDS-PAGE, in-gel trypsin digestion, and HPLC purification revealed a single radiolabeled peptide at fraction 36 (Figure 1A). To harvest the purified and labeled peptide in substantial amounts for mass spectrometric analysis, a cleavable biotinylated RCA analogue (**3**) was used to reveal the identity of the active site nucleophile. The biotin moiety of the reagent enables the facile purification of proteins labeled with it using a combination of tetravidin chromatography and elution at basic pH (17). In the latter step, the base-sensitive carboxyl ester moieties of BRCA (**3**) are cleaved, eluting the protein which is now labeled with a carboxymethylene moiety at the site of modification (Scheme 4). Labeling of tLRAT with BRCA (**3**) led to the results shown in Figure 1B. An avidin/ ECL blot (panel 1) showed the expected biotinylated protein at approximately 20 kDa. The SDS-PAGE blot showed the major 20 kDa protein, as did the Western blot. The faint bands that appear at 40 kDa are due to the tLRAT dimer. The labeled protein was treated with trypsin, and the biotinylated tLRAT peptide was purified by chromatography on a tetravidin column by a previously described method (17) (Figure 1B).

After the column was washed to remove unlabeled peptides, the base-sensitive biotinylated peptide was cleaved from the column at pH = 11, resulting in the modified peptide being tagged with a CH<sub>2</sub>CO<sub>2</sub>H fragment, which adds 58 Da (—H) to the modified peptide (17). Mass spectrometric analysis of the peptide readily identified C161 as the modified amino acid, thus consequently identifying this residue as the active site nucleophile of tLRAT. The biotinylated tLRAT peptide labeled with BRCA (3) was analyzed by ESI MS/MS to show two modified peptides (WNNC#EHFVTYCRYGTPISPQSDKF, MW = 2952.2080, and NNC#EHFV, MW = 920.9354). C# represents the modified Cys residue (MW + 58). To make absolutely sure that the labeling by BRCA identified the correct Cys residue, the labeling was repeated using BACMK (4), the reagent used initially for the identification of LRAT (7). BACMK inactivates LRAT, like the structurally dissimilar BRCA. BACMK labeling of tLRAT followed by SDS-PAGE, in-gel trypsin digestion, and avidin column purification using 8 M guanidine hydrochloride elution, C18 column purification, and MALDI-TOF mass spectrometry analysis showed one peptide of MW = 1315 which represents NNCEHF (763) + BACMK – Cl – Boc (552) (Figure 1C). The Boc moiety is lost as a consequence of TFA treatment, and Cl is lost as a consequence of alkylation. Thus, BACMK (4) has labeled the same C161 as BRCA (3). These direct labeling experiments establish C161 as the active site nucleophile.

#### H60 as the Essential His Residue of LRAT

As mentioned above, of the six His residues of LRAT, only H60 is uniquely conserved. Previous studies had shown that H46Q, H72Q, and H126Q are all active in full-length human LRAT (15). H163Q proved to be inert in this series, probably because of its proximity to C161, the active site Cys. H163 is not fully conserved in this family whereas H60 is, showing that H163 is unlikely to be essential for catalysis. Previous studies (15) suggesting the importance of H57 instead of H60 for catalysis were occasioned by problems in cloning. Resequencing of the H57Q and H60Q LRAT clones that we were sent unfortunately showed them to be in error. To clarify which of the remaining His residues, H57 or H60, is essential for catalysis, the H57Q and H60Q mutations were made in both tLRAT and full-length LRAT (Figure 2). Kinetic analysis of the mutants clearly indicates that H60, the conserved His residue in the LRAT family, not H57, is essential for catalysis both in LRAT and in tLRAT. Thus coupled with C161, H60 forms the minimal catalytic dyad of LRAT.

#### Site-Specific Mutagenic Studies on Q177 and D67

The experiments reported above demonstrate that the conserved residues C161 and H60 are essential for catalysis by LRAT. In addition to these two residues, which are absolutely conserved in the family of homologues, Q177 and D67 are generally conserved in the family of homologues. Of the remaining Gln residues in the LRAT family, only Q177 is conserved. However, of the LRAT isoform Asp residues, D49, D76, D111, D128, and D191 are conserved. As mentioned previously, Gln and Asp residues are often found to be important as catalysts in thiol proteases. Thus LRAT mutations at Q177, D67, D49, D76, D111, D128, and D191 were explored (Figure 3, Table 1). When probed by mutagenic studies, Q177E proved to be marginally active ( $1.0 \pm 0.2 \text{ mmol min}^{-1} \text{ mol}^{-1}$ , 6% compared to WT) in tLRAT, but Q177S shows considerably more activity ( $11.8 \pm 1.2 \text{ mmol min}^{-1} \text{ mol}^{-1}$ , 72%

compared to WT). Thus Q177 is not essential catalytically in LRAT. The one generally conserved Asp67 in the LRAT family appears unimportant for catalysis inasmuch as D67A is quite active (Figure 3). The remaining D → N mutants were active, showing that these Asp residues are not essential for catalysis even in the restricted LRAT series.

## DISCUSSION

The experiments described here were designed to define the catalytic residues of LRAT. The work is guided by the conserved sequences observed in the LRAT family (Scheme 3). It is shown here that the conserved residues C161 and H60 are essential for catalysis. Previous studies by site-specific mutagenesis had shown that both C161 and C168 were important for catalysis but that only C161S is inactive while C168S is substantially active (14). This latter result and the active site labeling experiments reported, with two structurally different reagents, here leave little doubt that it is C161 which is the active site nucleophile of LRAT. Any role for C168 in catalysis is of a secondary importance. The essential catalytic dyad of Cys and His in LRAT is reminiscent of the catalytic dyad of the thiol proteases (18–20).

In thiol proteases, additional residues, such as Asp and Asn, may also contribute to catalysis as well (21, 22). Thiol proteases can also have a catalytically significant Gln residue which forms part of the oxyanion hole (18–22). The additional fact that the viral and bacterial homologues (23) of LRAT are likely to be proteases further suggests that LRAT may be mechanistically related to thiol proteases. Kinetic analysis supports this view (24). Kinetically, LRAT operates by an ordered ping-pong kinetic mechanism with lecithin binding first (24), followed by the transfer of an *sn*-1 acyl group to C161. After lysolecithin departs, vitamin A binds and accepts the acyl moiety, producing an all-*trans*-retinyl ester. The overall reaction mechanism for LRAT, consistent with the known kinetic and biochemical data, is shown in Scheme 1.

This mechanism is also similar to a thiol protease mechanism and essentially differs in that in proteases the acyl-enzyme intermediate is attacked by water as the accepting nucleophile, rather than by vitamin A in the case of LRAT. However, if LRAT possesses a thiol protease motif, it must be novel for several reasons. First, LRAT shows no homology in the usually conserved residues propinquous to the essential Cys and His in any of the approximately 20 families of thiol proteases (25). Second, LRAT does not appear to contain catalytically essential Gln or Asp residues. While the LRAT family contains a largely conserved Q177, this residue can be readily substituted by serine with little effect on catalytic activity. The fact that Q177S is rather active in tLRAT suggests that inasmuch as there is a requirement at position 177 it is for a neutral polar residue rather than being specifically for glutamine. By way of comparison, in thiol proteases which contain a catalytically significant Gln, the mutation to Ser has a large negative effect on catalysis (26). In the Asp series, only D67 is largely conserved in the global LRAT family. However, D67A is still considerably active in tLRAT. The remaining Asp residues that are conserved in the specific LRAT family are also clearly not essential, because the remaining D → N mutations are active. Finally, LRAT exhibits  $pK_A$ 's of 8.3 and 10.8 in its pH vs rate profile (14), while thiol proteases exhibit  $pK_A$ 's of approximately 4.0 and 8.5 (18–20). In the thiol proteases the  $pK_A$  of 4.0 is attributed to the active site Cys, while the  $pK_A$  of 8.5 is attributed to the essential His residue

(27). It is unclear to which residues the two  $pK_A$ s of LRAT are attributed, but the studies described here show that the higher  $pK$  probably cannot be attributed to Q177.

Given the results described above, we believe therefore that LRAT represents a new mechanistic class of enzymes, which, while possibly related to thiol proteases, is clearly dissimilar in many important respects. It is also interesting to note that LRAT is homologous to proteins which are not easily recognized as protease candidates, such as class II tumor suppressors (9, 10) and EGL-26, a putative enzyme that mediates vulval cell morphogenesis in *C. elegans* (12). It will be of interest to determine if these latter proteins possess acyltransferase activities.

## References

1. Fulton B, Rando RR. *Biochemistry*. 1987; 26:7938–7945. [PubMed: 3427115]
2. MacDonald PN, Ong DE. *J. Biol. Chem.* 1988; 263:12478–12482. [PubMed: 3410848]
3. Saari JC, Bredberg DL. *J. Biol. Chem.* 1989; 264:8636–8640. [PubMed: 2722792]
4. Rando RR. *Chem. Rev.* 2001; 101:1881–1896. [PubMed: 11710234]
5. Zolfaghari R, Ross AC. *J. Lipid Res.* 2000; 41:2024–2034. [PubMed: 11108736]
6. Barry RJ, Cañada FJ, Rando RR. *J. Biol. Chem.* 1989; 264:9231–9238. [PubMed: 2722827]
7. Ruiz A, Winston A, Lim Y-H, Gilbert BA, Rando RR, Bok D. *J. Biol. Chem.* 1999; 274:3834–3841. [PubMed: 9920938]
8. Shi Y-Q, Furuyoshi S, Hubacek I, Rando RR. *Biochemistry*. 1993; 32:3077–3080. [PubMed: 8457568]
9. Sers C, Emmenegger U, Husmann K, Bucher K, Andres AC, Schafer R. *J. Cell Biol.* 1997; 136:935–944. [PubMed: 9049257]
10. Hajnal A, Klemenz R, Schafer R. *Oncogene*. 1994; 9:479–490. [PubMed: 8290259]
11. Hughes PJ, Stanway G. *J. Gen. Virol.* 2000; 81:201–207. [PubMed: 10640559]
12. Hanna-Rose W, Han M. *Dev. Biol.* 2002; 241:247–258. [PubMed: 11784109]
13. Bok D, Ruiz A, Yaron O, Jahng WJ, Ray A, Xue L, Rando RR. *Biochemistry*. 2003; 42:6090–6098. [PubMed: 12755610]
14. Mondal MS, Ruiz A, Bok D, Rando RR. *Biochemistry*. 2000; 39:5215–5220. [PubMed: 10819989]
15. Mondal MS, Ruiz A, Hu J, Bok D, Rando RR. *FEBS Lett.* 2001; 489:14–18. [PubMed: 11231005]
16. Nesnas N, Rando RR, Nakanishi K. *Tetrahedron*. 2002; 58:6577–6584.
17. Jahng WJ, David C, Nesnas N, Nakanishi K, Rando RR. *Biochemistry*. 2003; 42:6159–6168. [PubMed: 12755618]
18. Storer AC, Ménard R. *Methods Enzymol.* 1994; 244:486–500. [PubMed: 7845227]
19. Mellor GW, Thomas EW, Topham CM, Brocklehurst K. *Biochem. J.* 1993; 290:289–296. [PubMed: 8439297]
20. Salih E, Malthouse JPG, Kowlessur D, Jarvis M, O’Driscoll M, Brocklehurst K. *Biochem. J.* 1987; 247:181–193. [PubMed: 2825655]
21. Ménard R, Khouri HE, Plouffe C, Laflamme P, Dupras R, Vernet T, Tessier DC, Thomas DY, Storer AC. *Biochemistry*. 1991; 30:5531–5538. [PubMed: 2036422]
22. Vernet T, Tessier DC, Chatellier J, Plouffe C, Lee TS, Thomas DY, Storer AC, Ménard R. *J. Biol. Chem.* 1995; 270:16645–16652. [PubMed: 7622473]
23. Anantharaman V, Aravind L. *Genome Biol.* 2003; 4:R11–R11.12. [PubMed: 12620121]
24. Shi Y-Q, Hubacek I, Rando RR. *Biochemistry*. 1993; 32:1257–1263. [PubMed: 8448136]
25. Rawlings ND, Barrett AJ. *Methods Enzymol.* 1994; 244:461–486. [PubMed: 7845226]
26. Dufour E, Storer AC, Ménard R. *Biochemistry*. 1995; 34:9136–9143. [PubMed: 7619812]
27. Storer AC, Ménard R. *Methods Enzymol.* 1994; 244:486–500. [PubMed: 7845227]



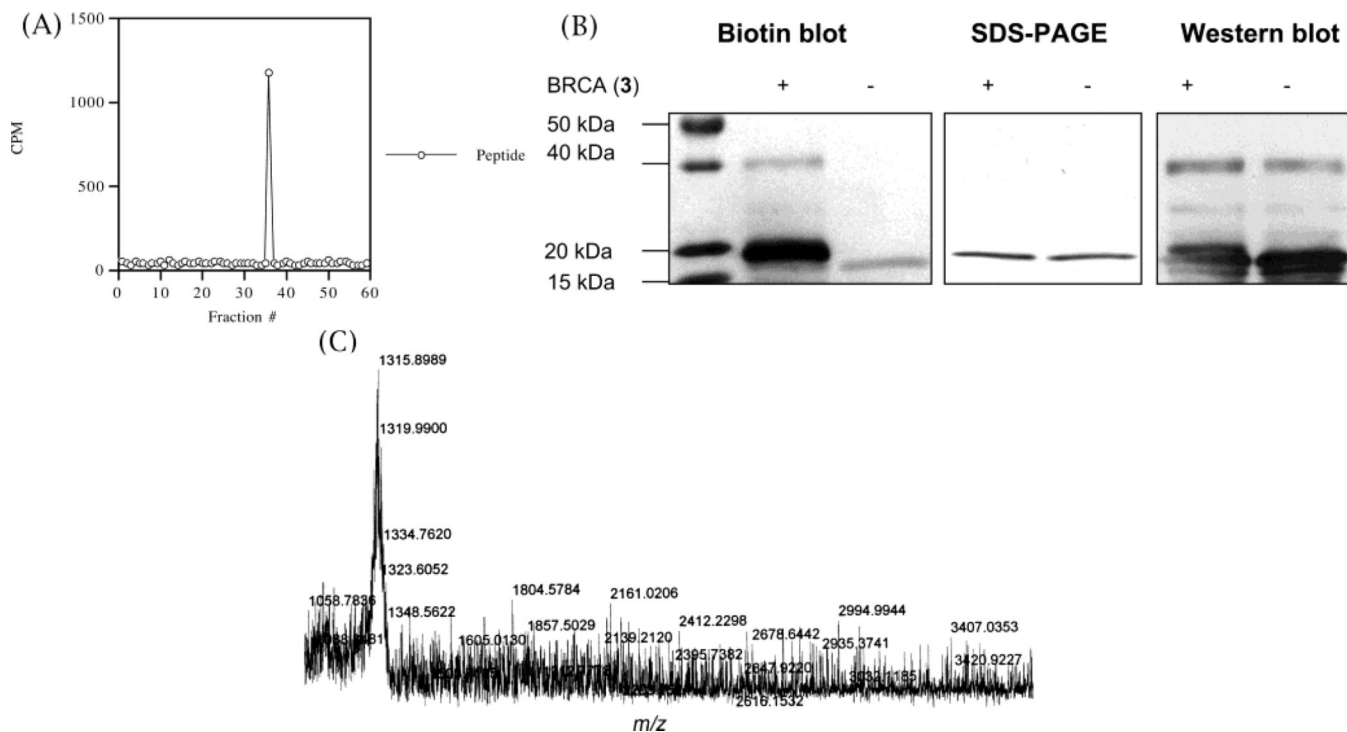


**Figure 1.** tLRAT labeling by affinity labeling reagents. (A) HPLC chromatogram of [11,12-<sup>3</sup>H<sub>2</sub>]RCA (2) labeled tLRAT peptide. RPHPLC was performed on a microcapillary C18 column (Vydac 218TP52). The peptides were eluted with a linear gradient from 0 to 70% acetonitrile with 0.1% TFA. Fractions were collected every minute (50 μL), and radioactivity was monitored by scintillation counting (Beckman LS6500) using Ultima Gold scintillation cocktail. (B) tLRAT labeling by alkali-cleavable affinity reagent BRCA (3). tLRAT was visualized by Coomassie blue staining, Western blot by anti-LRAT antibody/anti-rabbit Ig-HRP/ECL, and biotin blot by avidin-HRP/ ECL. The 40 kDa band represents the tLRAT homodimer. (C) MALDI TOF analysis of the BACMK (4) labeled tLRAT peptide. One peptide (MW = 1315) represents NNCEHF (763) + BACMK - Cl - Boc (552).

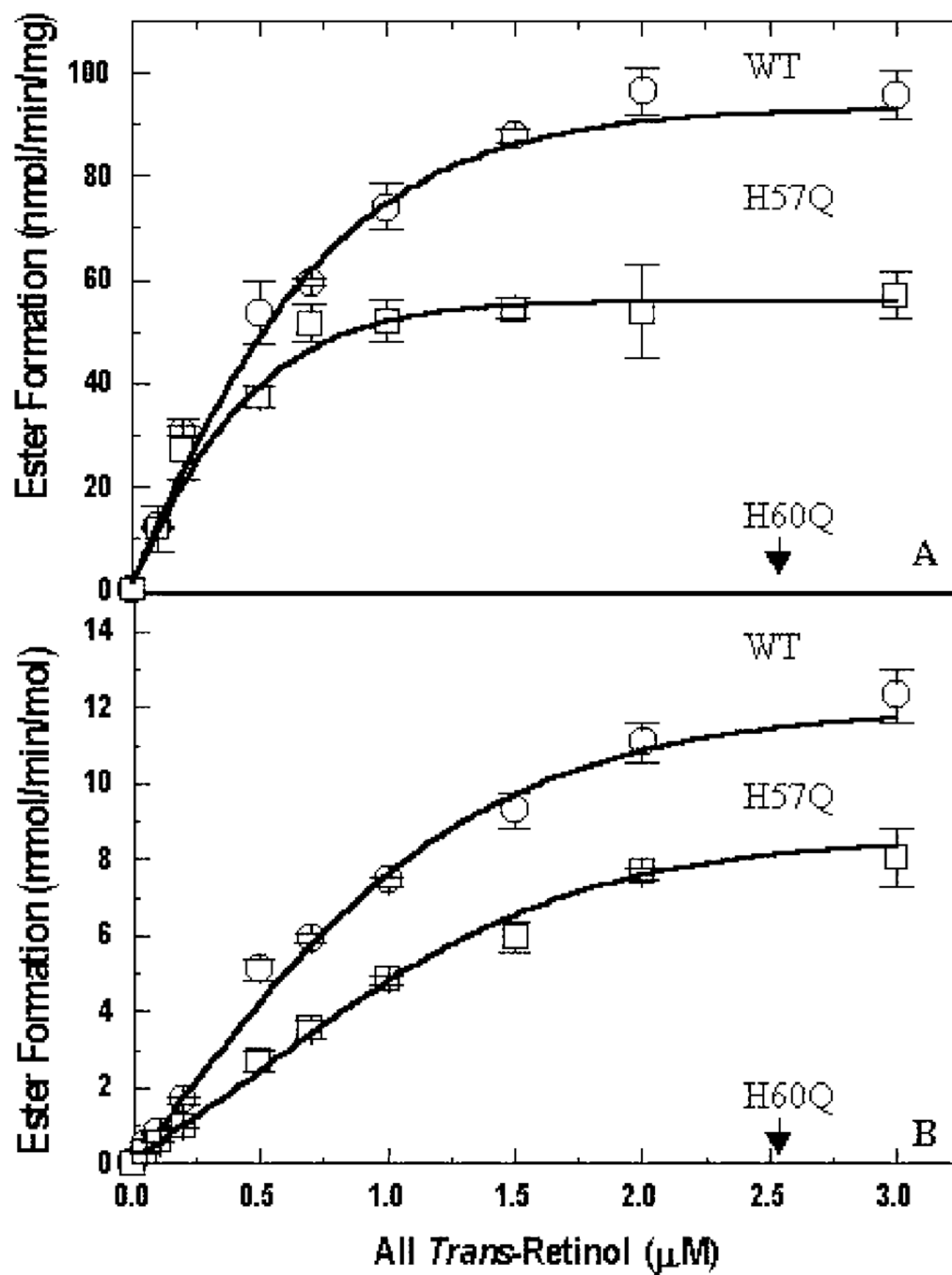


**Figure 2.** Steady-state kinetic analysis of LRAT. Retinyl ester formation by WT LRAT (○) and H57Q (□) is shown. The same numbering system based on full-length LRAT is used for tLRAT as well to avoid confusion. (A) Full-length LRAT and the mutants. H57Q and H60Q mutants were generated by the overlapping extension method. Expression and membrane protein preparation were performed as described in Methods. The calculated  $V_{\max}$  values of WT and H57Q are  $122.58 \pm 4.92$  and  $67.50 \pm 3.65$   $\text{nmol min}^{-1} \text{mg}^{-1}$ , respectively. The  $K_M$ s are  $0.65 \pm 0.03$  and  $0.29 \pm 0.08$   $\mu\text{M}$ , respectively. (B) tLRAT and the mutants. Mutagenesis was

conducted using the QuikChange site-directed mutagenesis kit (Stratagene Inc.). The  $V_{\max}$  values of tLRAT and H57Q are  $16.41 \pm 0.38$  and  $12.70 \pm 0.67$   $\text{mmol min}^{-1} \text{mol}^{-1}$ , respectively. The  $K_M$ s are  $1.67 \pm 0.24$  and  $2.73 \pm 0.37$   $\mu\text{M}$ , respectively. No activity was observed in H60Q and the empty vectors in both (A) and (B).

Author Manuscript

Author Manuscript

Author Manuscript

Author Manuscript

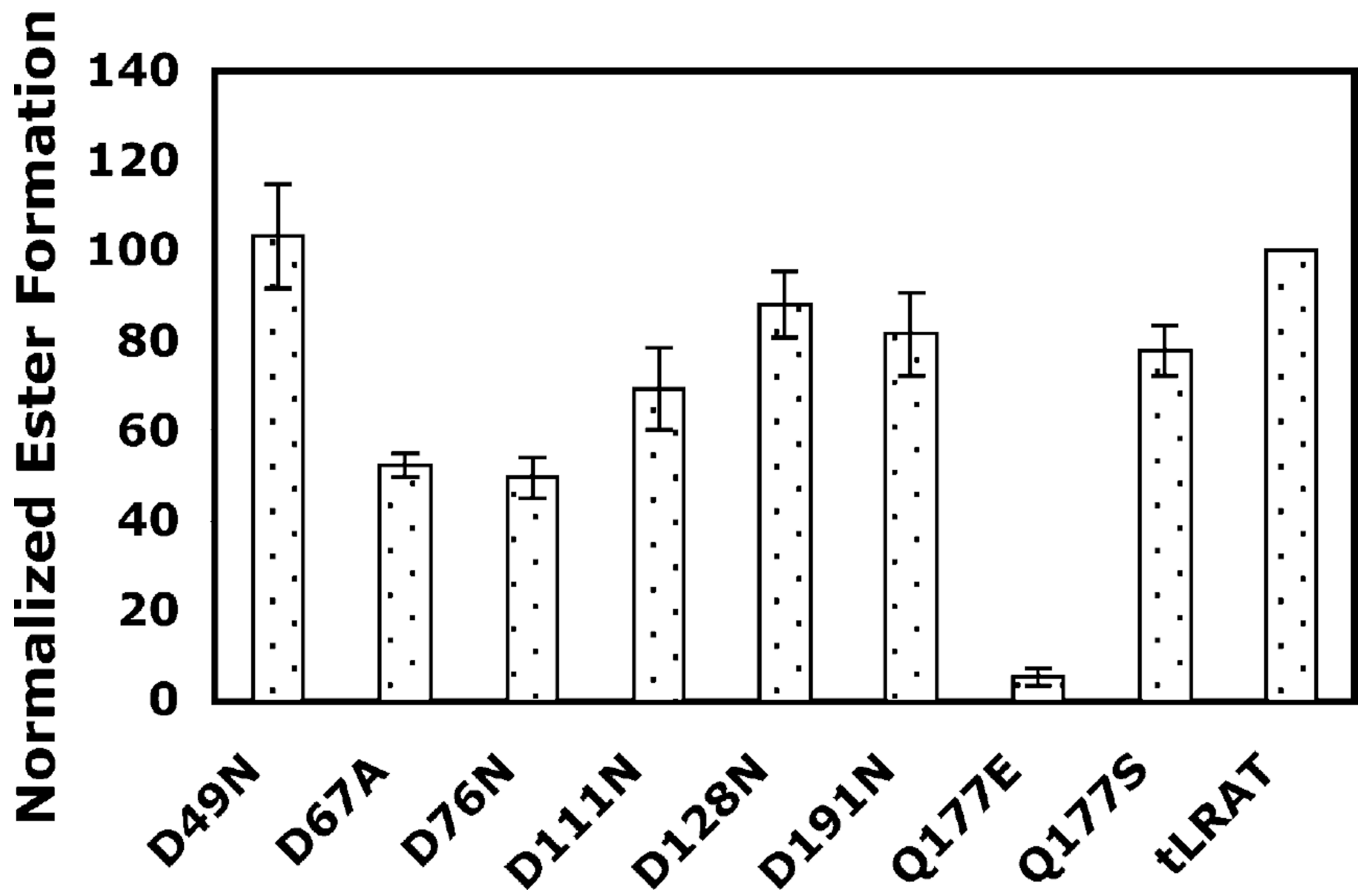
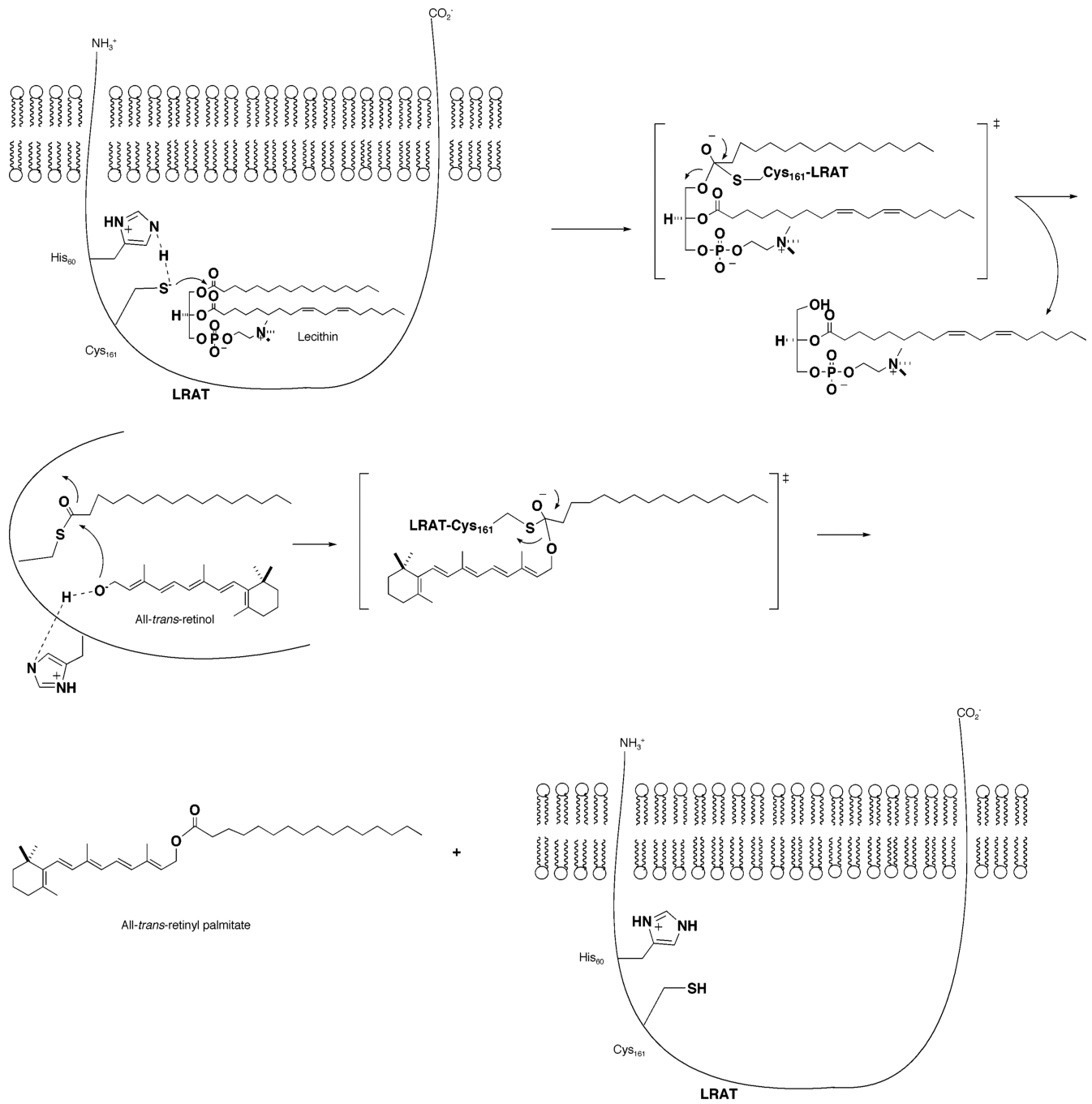
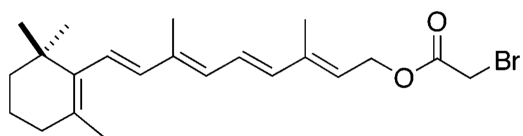


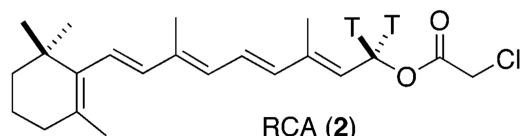
**Figure 3.** Normalized all-*trans*-retinyl ester formation by tLRAT mutants using all-*trans*-retinol as substrate. Esterification activity of tLRAT was monitored by following the formation of all-*trans*-retinyl esters using  $^3\text{H}$ -labeled all-*trans*-retinol ( $0.2 \mu\text{M}$ ) along with DPPC ( $220 \mu\text{M}$ ), 0.6% BSA (0.6%), EDTA (1 mM), DTT (2 mM), and CHAPSO (0.1%) in Tris buffer (100 mM, pH 8.3). The values are the average of triplicate measurements.



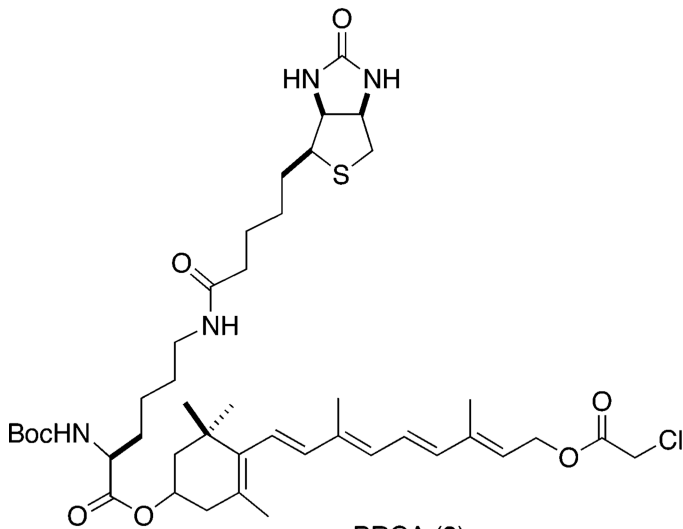
**Scheme 1.**  
LRAT Mechanism



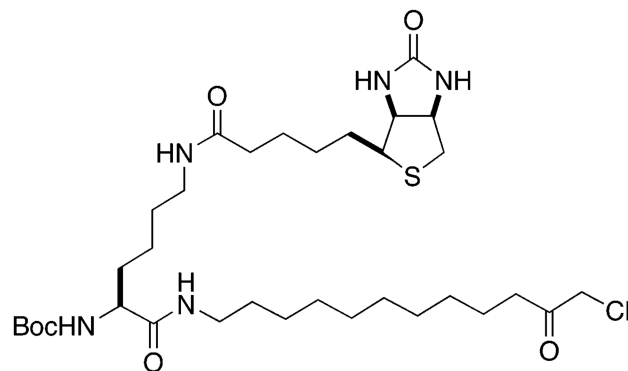
RBA (1)



RCA (2)



BRCA (3)



BACMK (4)

**Scheme 2.**  
Affinity Labeling Reagents of LRAT

Human-LRAT	-MKNPMLEVVSLLEKLLLSNFTLFSGGAAGKDKGRNSFYETS-SFHRG 48
Bovine-LRAT	-MKNPMLEAVSLVLEKLLFISYFKFFSSGAPGQDKAGNTLYEIS-SFLRG 48
Mouse-LRAT	-MKNPMLEAASLLEKLLLSNFKLFSVVPGGGTGNRPFYEIS-SFVRG 48
Rat-LRAT	-MKNMLEAASLLEKLLLSNFKLFSVVPGGGTGKHPYEIN-SFLRG 48
XL-LRAT	-MKSLLVGMVIFPEKIFILANLKVFSVSS--KKSRCRQPCNVP-PIKRG 46
ZF-LRAT	-----MLDSLLEKLLTLLAHNFFSFTSSKQERCTRREISTYFQRG 45
HRev107-Mouse	-----MLAPIPEP---KPG 11
HRev107-RAT	-----MPIPEP---KPG 9
HRev107-3	-----MRAPIPEP---KPG 11
TIG3	-----MASPHQEP---KPG 11
Echovirus23	KIEVYLSLRCPNLFPPSPAPKEKTSRALRGLDANFIQSPYGGQQQTQMM 53
HumanParechovirus1	-----LSLRCPNFFPLPAPKVTSSRALRGMANLTNQSFPYGGQQPNRM 45
HumanParechovirus2	-----LSLRCPNFFPLPAPKP-ATRKYRGDLATWSQSPYGRGQKQLM 44
Avian-encephalomyelitis-virus	-----KTMVNTYWLDDDELVESSHSSPDEIEEAQCSCKMDLG 39
EGL26	RLTTVLGRPGMFSFDDPPIGSQPFVKGELIQLDEVPVGVHQRDKYLEKG 150
Aichivirus	-----TPDVDP----- 6
Human-LRAT	D---VLEVPRTHLTHYGIYLGDNVAHMPDILLALTDMDGRTQKVVSN 94
Bovine-LRAT	D---VLEVPRTHLTHYGIYLGDNVAHMPDILLALTDKGRQTKVVSN 94
Mouse-LRAT	D---VLEVSRTHFIHYGIYLGDNVAHMPDILLALTDKERTQKVVSN 94
Rat-LRAT	D---VLEVSRTHFIHYGIYLGDNVAHMPDILLALTDKERTQKVVSN 94
XL-LRAT	D---LLEVPRTLFVHFGIYLGDNVAHMPDILPALSDTCLIRRVVITN 92
ZF-LRAT	D---LLEVPRTLFVHFGIYLGDNVAHMPDILPVLTSNKHQLNVVITN 91
HRev107-Mouse	D---LIEIFRPMYRHWAIVYGDGYVHILAPPSEVAGAGAAS----- 49
HRev107-RAT	D---LIEIFRPMYRHWAIVYGDGYVHILAPPSEVAGAGAAS----- 47
HRev107-3	D---LIEIFRPMYRHWAIVYGDGYVHILAPPSEVAGAGAAS----- 49
TIG3	D---LIEIFRPMYRHWAIVYGDGYVHILAPPSEVAGAGAAS----- 49
Echovirus23	K---LAYLDRGFYKHYGIYVGDGYVYQLDSDIFKTA----- 86
HumanParechovirus1	K---LAYLDRGFYKHYGIYVGDGHVYQLDSDIFKTA----- 78
HumanParechovirus2	K---LAYLDRGFYKHYGIYVGDGHVYQLDSDIFKTA----- 77
Avian-encephalomyelitis-virus	D---IVSCEGKAKHFGYVYVGDGVDVHVDPEGNATNWFMKR----- 76
EGL26	DEVFCEVNVSGVKVYHSGIYAGDGMCYHFVCDQAQESSEFADALAVFSG-- 198
Aichivirus	D---DRVYIVRAQRPTYVHWARKVAPDGSAAKISLSRSGIQALV----- 48
Human-LRAT	KRLILGVIVKVASIRVDVDFAYGANILVNHLEDSLQKALLNNEVARR 144
Bovine-LRAT	KRLILGVIVKVASIRVDVDFAYGAEILVNHLDRLSKKALLNNEVARR 144
Mouse-LRAT	KRLILGVIVKVASIRVDVDFAYGADILVNHLDGTLKSKALLNNEVARR 144
Rat-LRAT	KRLILGVIVKVASIRVDVDFAYGADILVNHLDGTLKSKALLNNEVARR 144
XL-LRAT	KRLIMGVLAIASIRVDVDFAYGNNILVNHMDKSFKTKPLTNEVARR 142
ZF-LRAT	KRLILGVLYKIASIRVDVDFAYGNNILVNHMDTLRQKPLAAEVARR 141
HRev107-Mouse	---IMSALTDKAIKVKELLCHVAGKQYQVNNKHDEEYTP-PLPLSKIIQR 95
HRev107-RAT	---IMSALTDKAIKVKELLRDVAGKQYQVNNKHDEEYTP-PLPLNKIIQR 93
HRev107-3	---VMSALTDKAIKVKELLYDVAGSKYQVNNKHDDKYS-PLPCKSKIIQR 95
TIG3	---VFSVLSNSAEVGRLEDDVVGCCYRVNNSLDHEEYQ-PRPVEVIISS 95
Echovirus23	-----LTGKARFTKTRLTDPDWVVEECELDFRVKYLESSVNSEHIFS- 129
HumanParechovirus1	-----LTGKARFTKTRLTSDVWVEECELDFRKYKYLESSVNSEHIFS- 121
HumanParechovirus2	-----LTGKARFTKTRLTDPDWVVEECELDFRKYKYLESSVNSEHIFS- 120
Avian-encephalomyelitis-virus	-----KATVKKSKNLDKWCFAISPRIDRTLICETANLWVGRVEYD 117
EGL26	-----ASAHVVYDTWFEFVYALVEVDVPPKIFRASHPLICRSGEQVKY 243
Aichivirus	-----ALEPPEGEPEYLEILPSSHWTLAEALQGNKWEYS----- 93
Human-LRAT	AEKLLG-FTPYSLLNWNCHEFVTCRYGTPISPQSDKFCETVKIIIRDQR 193
Bovine-LRAT	AEKLLG-ITPYSLLNWNCHEFVTCRYGTPISPQADKFCENVKIIIRDQR 193
Mouse-LRAT	AEQQLG-LTPYSLLNWNCHEFVTCRYGSRISPQAEKFDYTVKIIIRDQR 193
Rat-LRAT	AEQQLG-LTPYSLLNWNCHEFVTCRYGSPISPQAEKFHETVKIIIRDQR 193
XL-LRAT	AEKLVG-STPY-LLWNCHEFVTCRYGMPVSPQTEKFCETVKIIIRDQR 190
ZF-LRAT	AEKLVG-HFTPYSLMWNWNCHEFVTCRYGTAVSLQTDQFCESLKSIIIRDQR 190
HRev107-Mouse	AERLVGQEVLYRLTSENCEHFVNELRYGVPRSDQ-----VRDAV 134
HRev107-RAT	AELVGVQEVLYRLTSENCEHFVNELRYGVPRSDQ-----VRDVT 132
HRev107-3	AELVGVQEVLYKLTSENCEHFVNELRYGVARSQD-----VRDVI 134
TIG3	AKEMVQKMKYSIVSRNCEHFVQALRYGKSRCKQ-----VEKAK 134
Echovirus23	-----VDSNCEETIAKDFIGTHLSQH-----QAI 153
HumanParechovirus1	-----VDKNCETIAKDFIGTHLSQH-----QAI 145
HumanParechovirus2	-----VDNNCETIAKDFIGSHLSQH-----QQI 144
Avian-encephalomyelitis-virus	-----IFVKNCEYARGIASDYGTEGEEK-----WKTLT 147
EGL26	AEHLQRELENYDIRRCNCQHSSECESTGVPPFSYD-----MTSMF 282
Aichivirus	A-----T-----NNCETHFVSSI-TGESLPN-----T 99
Human-LRAT	SVLASAVLGLASIVCTGLVSYTTLPAIIPFFLWMAG- 230
Bovine-LRAT	SVLASAVLGLASIFCLGLTSYTTLPALIPFFLWMAG- 230
Mouse-LRAT	SSLASAVLGLASIVYVGLASYMTLPAICIPFCLWMMMSG 231
Rat-LRAT	SCLASAVLGLVSIYVGLASYMTLPAVICIPFCLWMMMSG 231
XL-LRAT	SALLSAAIGMASVLCMFGGLCTILPFFIIPFTLWMAG- 227
ZF-LRAT	SILLTTVIGNLSMFPVGIAPSTALPFFIIPFILWMAG- 227
HRev107-Mouse	KAVGIVAGVLAALGLVGMVLSRNKKQKQ----- 162
HRev107-RAT	KVATVTGVLAAALGLVGMVLSRNKKQKQ----- 160
HRev107-3	IAASVAGMGLAAMSLIGVMSRNKKQKQ----- 162
TIG3	VEVGVA-TALGILVVGCSFARRRYQKATA----- 164
Echovirus23	GLVGAILLTAGLMTIKTPVNAITIKFFNHAIDGDEQ 191
HumanParechovirus1	GLVGTILLTAGLMTIKTPVNAVITIKFFNHAIDGDEQ 183
HumanParechovirus2	GLIGTILLTAGLMTIKTPVNPITIKFFNHAIDGDEQ 182
Avian-encephalomyelitis-virus	SAVGVAAMTTMMAMRHELLDTSITLTKLPKVGVEVT-- 182
EGL26	KYLACTVLPKPTSTVVNAMTRPNRDRSSPSSSTSS-- 317
Aichivirus	GFSLALGIGALTAIAASAVALKALPGRQGLLTLA 137

**Scheme 3.**

Multiple Sequence Alignment of the LRAT Family<sup>a</sup>

<sup>a</sup> Multiple sequence alignment of the LRAT family was performed by using CLUSTAL W 1.82 (<http://www.ebi.ac.uk/clustalw/>). Fully conserved His, Asn, and Cys are in red, the predicted transmembrane domain is in blue, and highly conserved Asn and Gln are in pink. Accession numbers are as follows: human LRAT (GP:AF 071510), bovine LRAT (GP:AF 275344), mouse LRAT (GP:AF 255061), rat LRAT (GP:AF 255060), mouse Hrev107 (AAH24581), rat Hrev107 (X76453), human Hrev107-3 (P53816), tazarotene-induced gene

protein (TIG3) (AF060228), echovirus 23, human parechovirus 1 (L02971), human parechovirus 2 (AJ005695), avian encephalomyelitis virus (AJ225173), EGL26 (NP493652), and aichivirus (AB010145).

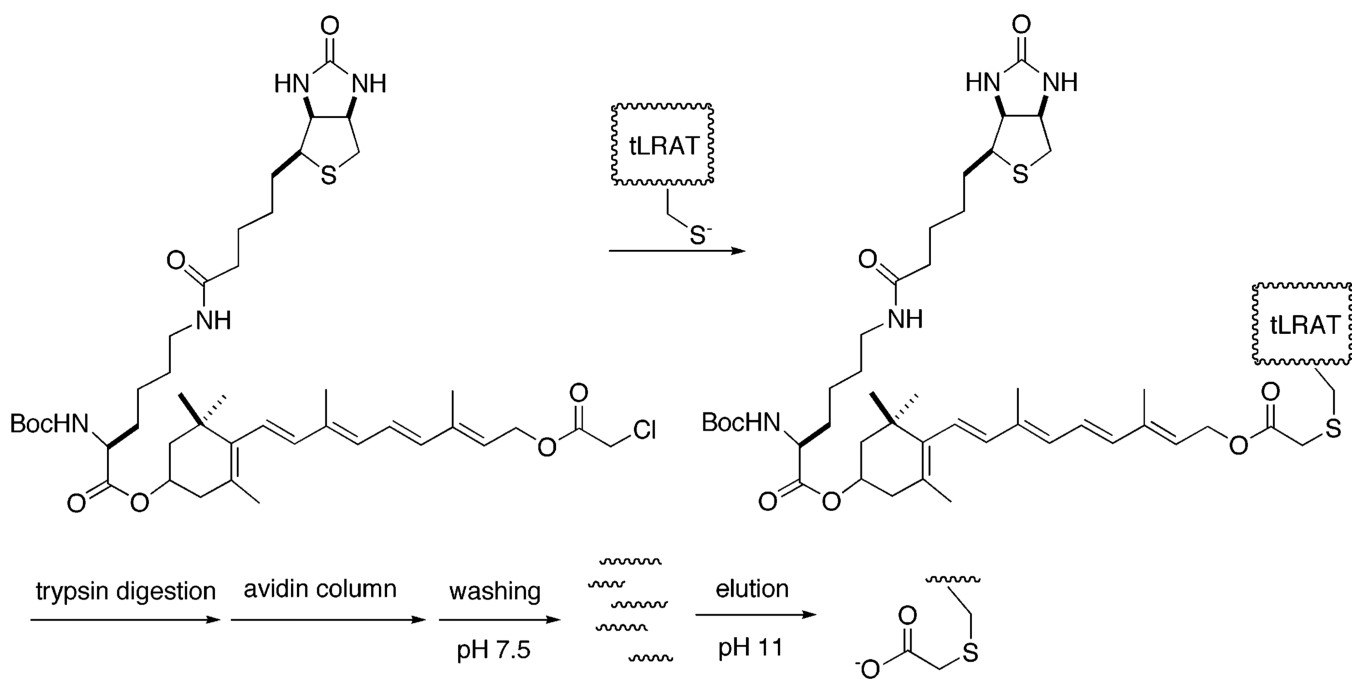
Author Manuscript

Author Manuscript

Author Manuscript

Author Manuscript





**Scheme 4.**  
Active Site Labeling of tLRAT by BRCA 3

**Table 1****Primers Used for Site-Directed Mutagenesis of tLRAT**

Q177S	(+): 5'-CCG ATC AGT CCC <b>TCG</b> TCC GAC AAG T-3'
	(-): 5'-A CTT GTC GGA <b>CGA</b> GGG ACT GAT CGG-3'
Q177E	(+): 5'-CCG ATC AGT CCC <b>GAG</b> TCC GAC AAG T-3'
	(-): 5'-A CTT GTC GGA <b>CTC</b> GGG ACT GAT CGG-3'
D49N	(+): 5'-C CAC CGA GGC <b>AAC</b> GTG CTG GAG GTG-3'
	(-): 5'-CAC CTC CAG CAC <b>GTT</b> GCC TCG GTG G-3'
D67A	(+): 5'-C ATC TAC CTA GGA <b>GCC</b> AAC CGT GTT GC-3'
	(-): 5'-GC AAC ACG GTT <b>GGC</b> TCC TAG GTA GAT G-3'
D76N	(+): 5'-CAC ATG ATG CCC <b>AAC</b> ATC CTG TTG GCC-3'
	(-): 5'-GGC CAA CAG GAT <b>GTT</b> GGG CAT CAT GTG-3'
D111N	(+): 5'-GC ATC CGC GTG <b>AAC</b> ACA GTG GAG GAC-3'
	(-): 5'-GTC CTC CAC TGT <b>GTT</b> CAC GCG GA T GC-3'
D128N	(+): 5'-GTC AAT CAC CTG <b>AAC</b> GAG TCC CTC CAG-3'
	(-): 5'-CTG GAG GGA C TC <b>GTT</b> CAG GTG AT T GAC-3'
D191N	(+): 5'-G ATA ATT ATT CGT <b>AAT</b> CAG AGA AGT GTT CTC-3'
	(-): 5'-C GAG AAC ACT TCT CTG <b>ATT</b> ACG AAT AA T TAT CG-3'